

Porosity Control in Pillar-Layered MOF Architectures: Hydrogen Bonding in Amino-Functionalized 2D Layers

Fatemeh Tavakoli-Quchani ^a, Alireza Salimi* ^a, and Ali Nakhaei Pour

^a Department of Chemistry, Faculty of Science, Ferdowsi University of Mashhad, Mashhad, Iran

* E-mail: salimi-a@um.ac.ir

Supporting Information

S0. List of Contents

Figure S0.	List of Contents	P.1
Figure S1.	The designed device for the FUMs synthesis.	P.2
Figure S2.	The FE-SEM images of (a) FUM-153(Zn-H) , (b) FUM-153(Zn-H)* , (c) FUM-167(Cd-H) , and (d) FUM-176(Cd-NH₂) .	P.2
Figure S3.	The overlay of PXRD plots of (a) FUM-153(Zn-H) , (b) FUM-167(Cd-H) , and (c) FUM-176(Cd-NH₂) .	P.3
Figure S4.	The FT-IR plot of (a) FUM-153(Zn-H) , (b) FUM-153(Zn-H)* , (c) FUM-167(Cd-H) , and (d) FUM-176(Cd-NH₂) .	P.5
Figure S5.	The TGA analysis of (a) FUM-153(Zn-H) , (b) FUM-167(Cd-H) , and (c) FUM-176(Cd-NH₂) .	P.4
Figure S6.	The DTA analysis of (a) FUM-153(Zn-H) , (b) FUM-167(Cd-H) , and (c) FUM-176(Cd-NH₂) .	P.8
Figure S7.	The representation of FT-SEM of FUM-153(Zn-H) and FUM-153(Zn-H)* .	P.8
Figure S8.	The representation of the 2-fold interpenetrating in FUM-153(Zn-H) .	P.9
Figure S9.	The representation of $\pi \cdots \pi$ interactions in FUM-153(Zn-H) .	P.9
Figure S10.	The representation of the 2-fold interpenetrating in FUM-167(Cd-H) .	P.10
Figure S11.	The representation of C40 O11 \cdots C47 N7 _{amide} and C29A O10A \cdots H52 C52 interactions interpenetrating in FUM-167(Cd-H) .	P.11
Figure S12.	The representation of the 2-fold interpenetrating in FUM-176(Cd-NH₂) .	P.11
Chart S1.	CH ₄ and CO ₂ gas adsorption result in the three FUMs.	P.11
Table S1.	The calculated gas adsorption results of all FUMs.	P.12

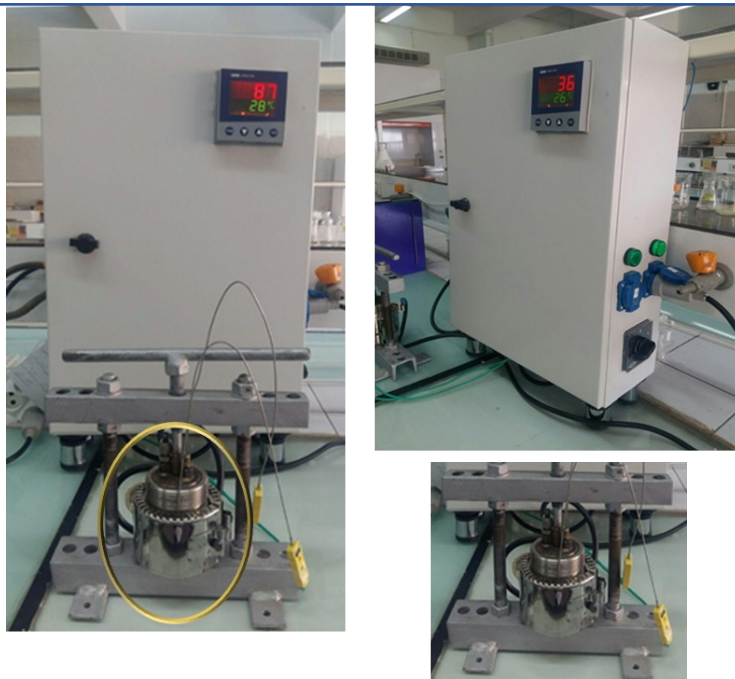


Figure S1. The designed device for the FUMs synthesis.

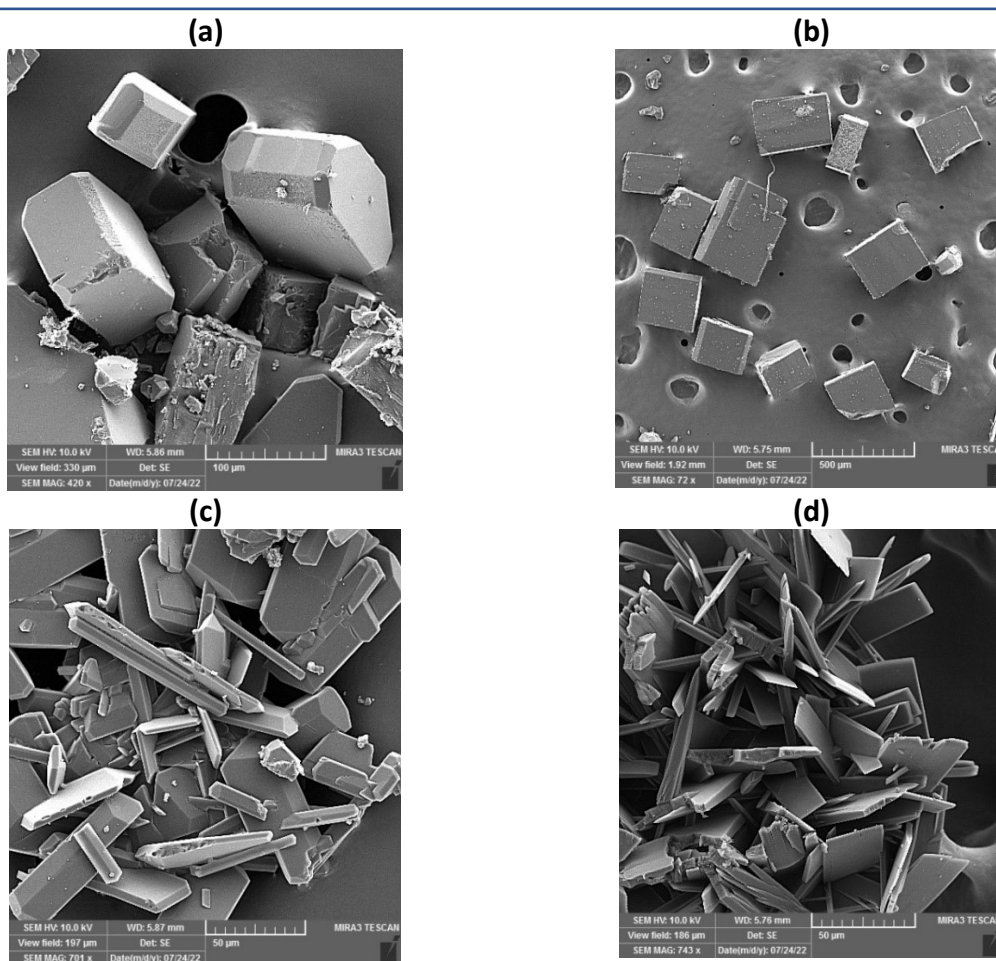


Figure S2. The FE-SEM images of (a) FUM-153(Zn-H), (b) FUM-153(Zn-H)*, (c) FUM-167(Cd-H), and (d) FUM-176(Cd-NH₂).

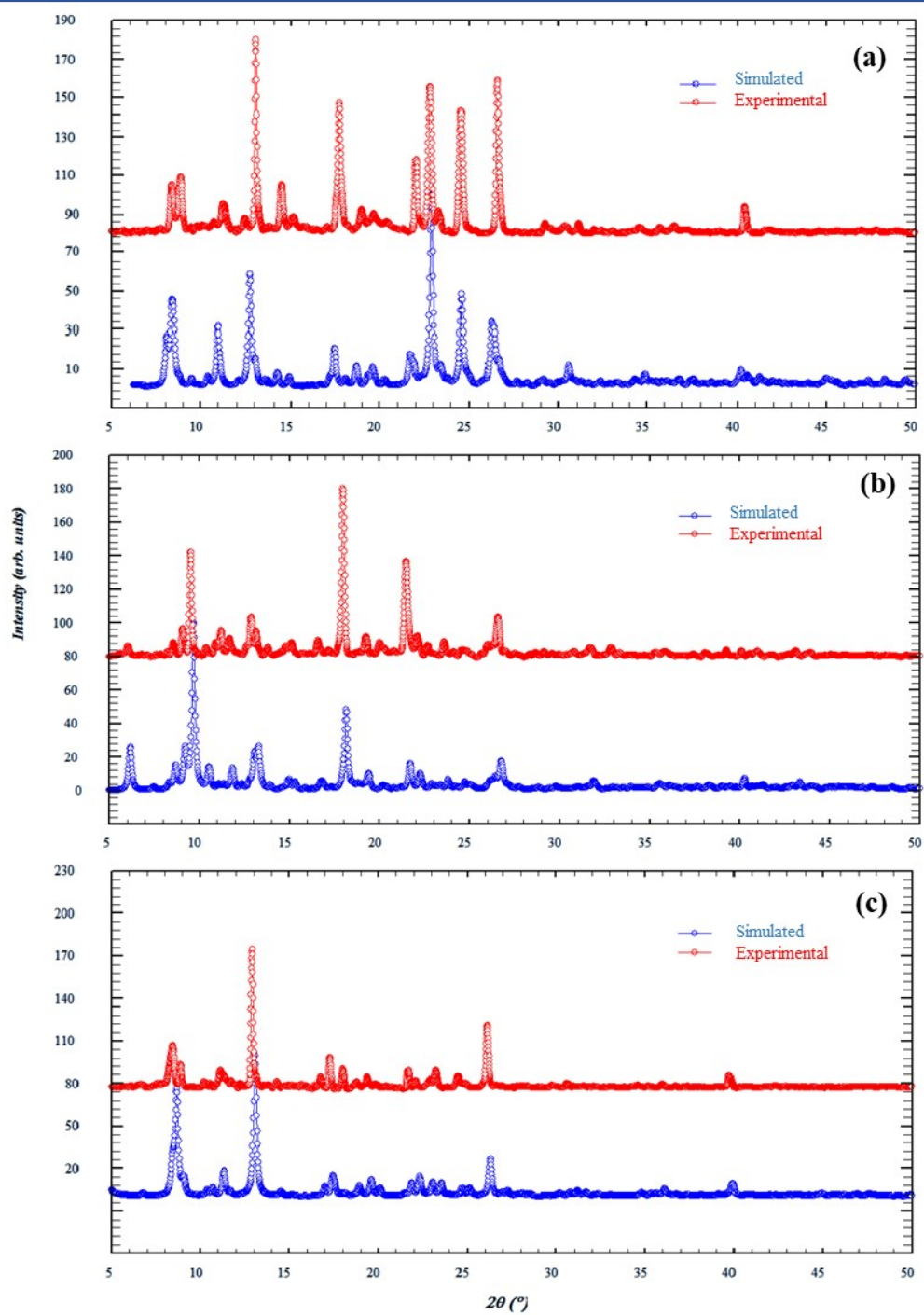
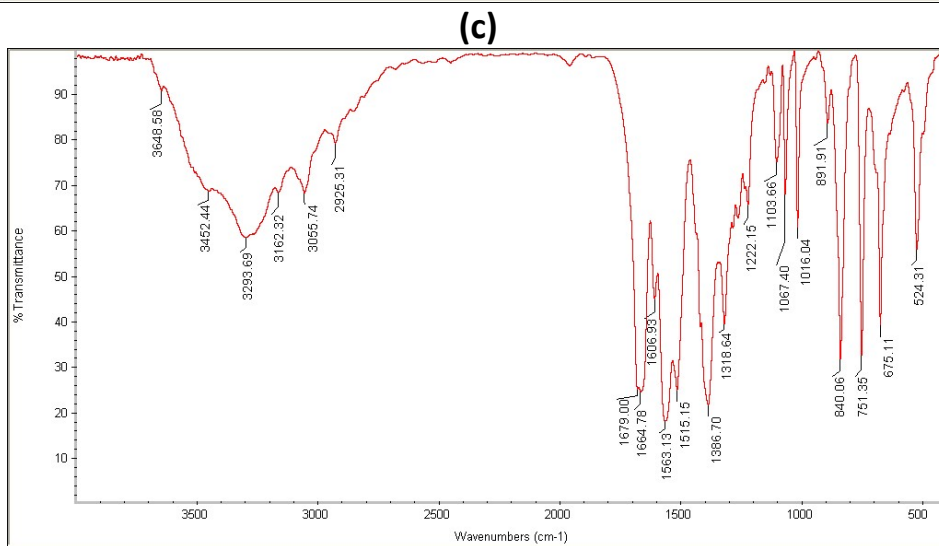
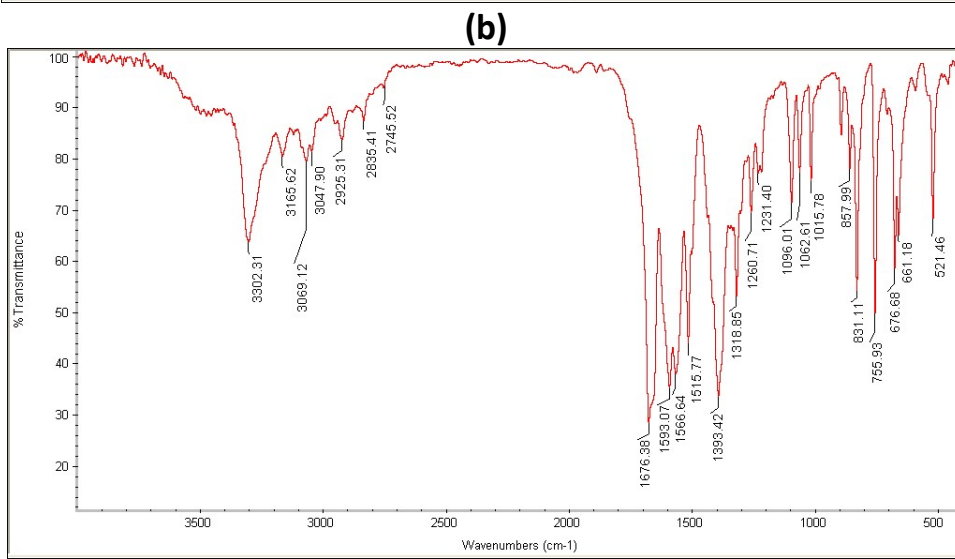
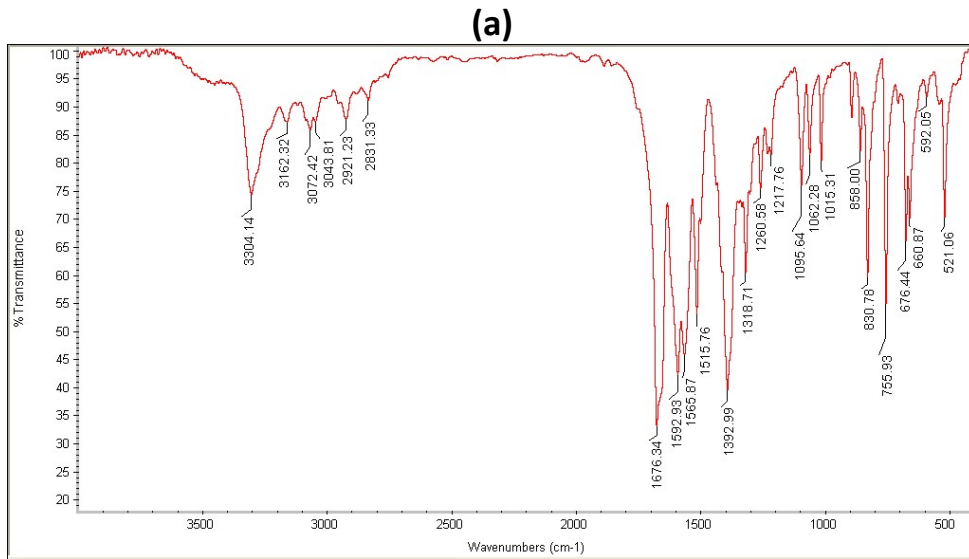


Figure S3. The overlay of PXR D plots of (a) FUM-153(Zn-H), (b) FUM-167(Cd-H), and (c) FUM-176(Cd-NH₂).



(d)

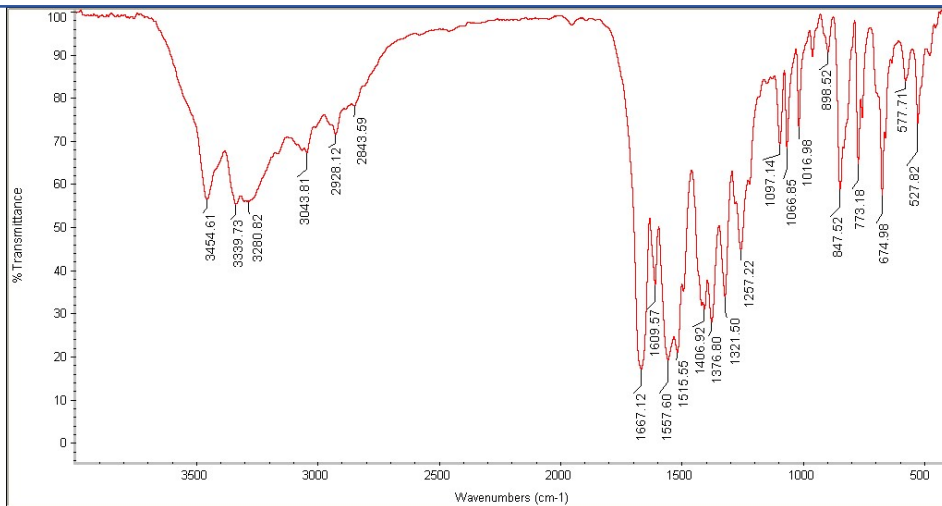
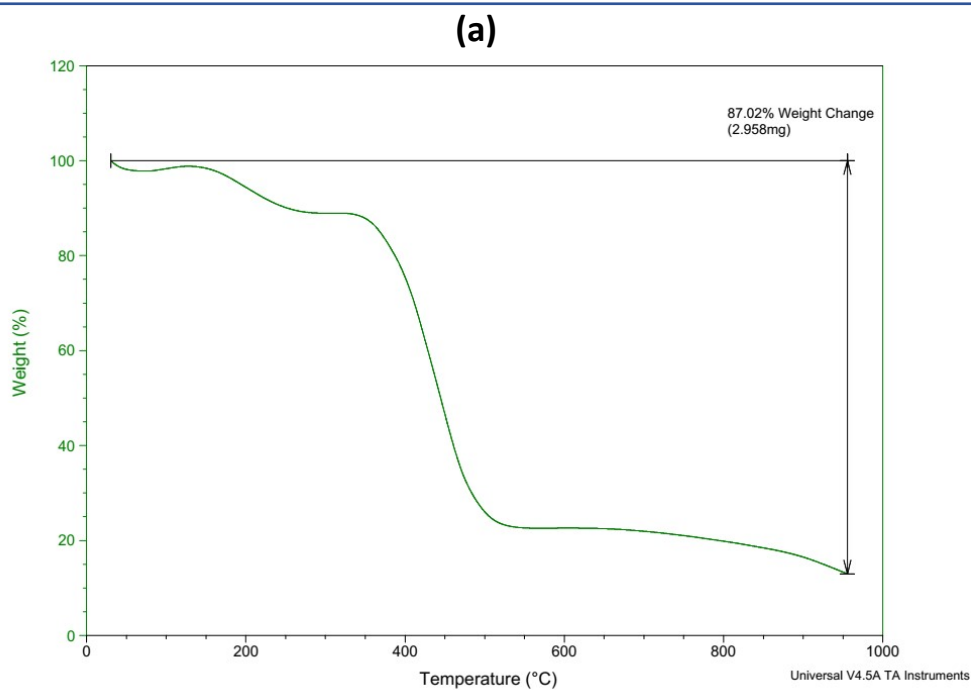
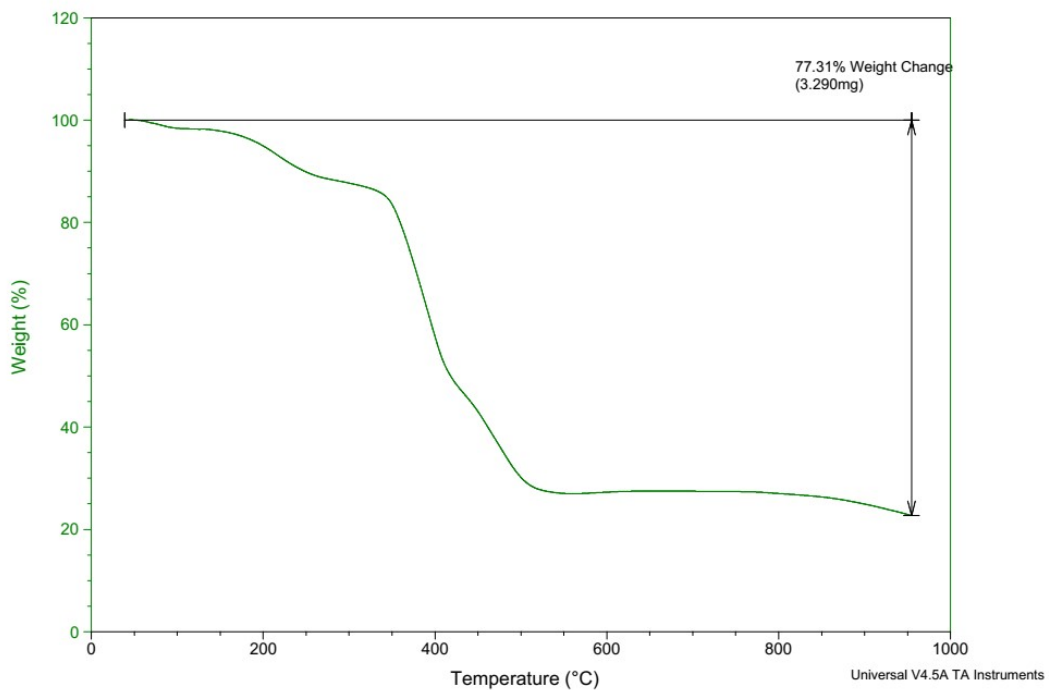


Figure S4. The FT-IR plot of (a) FUM-153(Zn-H), (b) FUM-153(Zn-H)*, (c) FUM-167(Cd-H), and (d) FUM-176(Cd-NH₂).



(b)



(c)

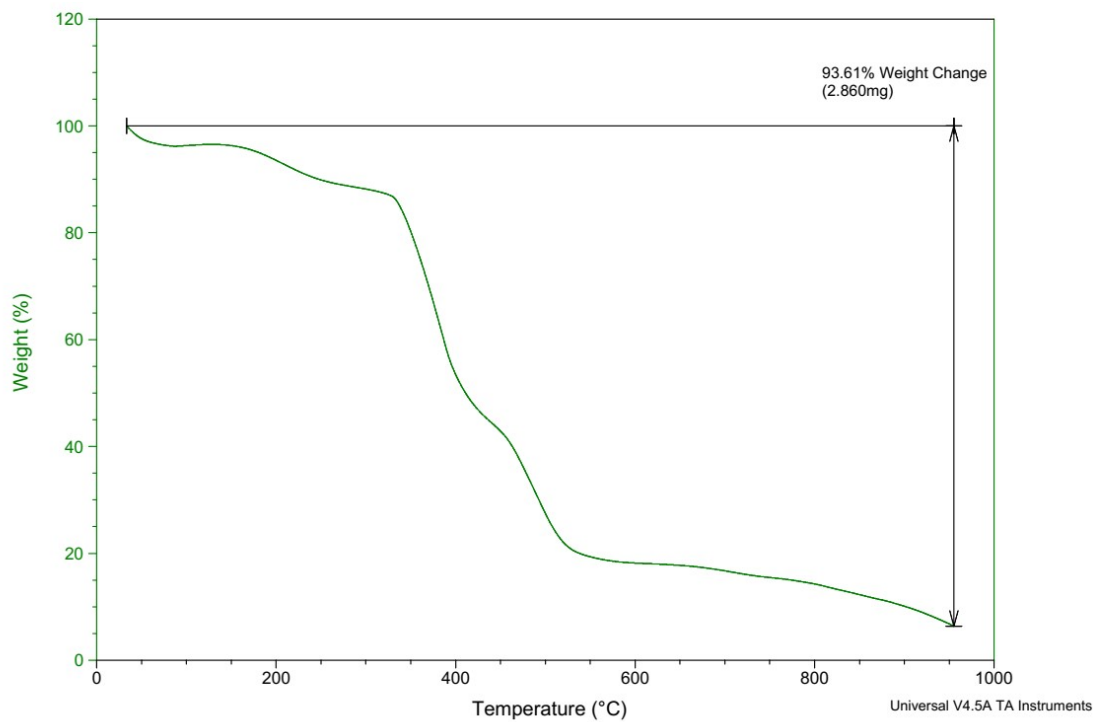
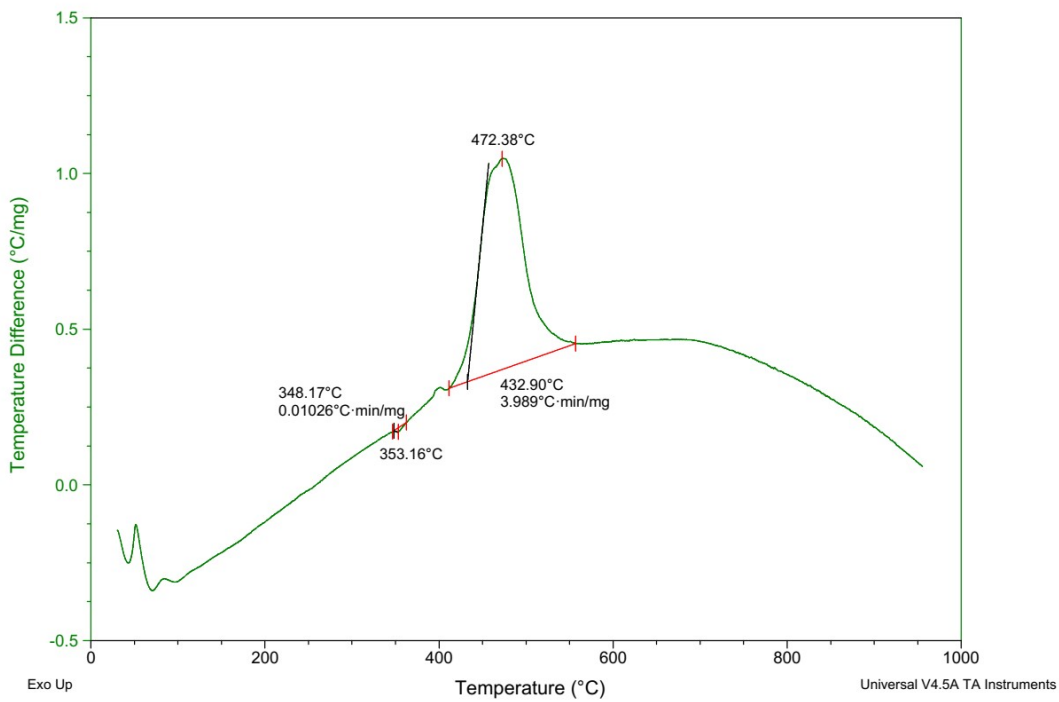
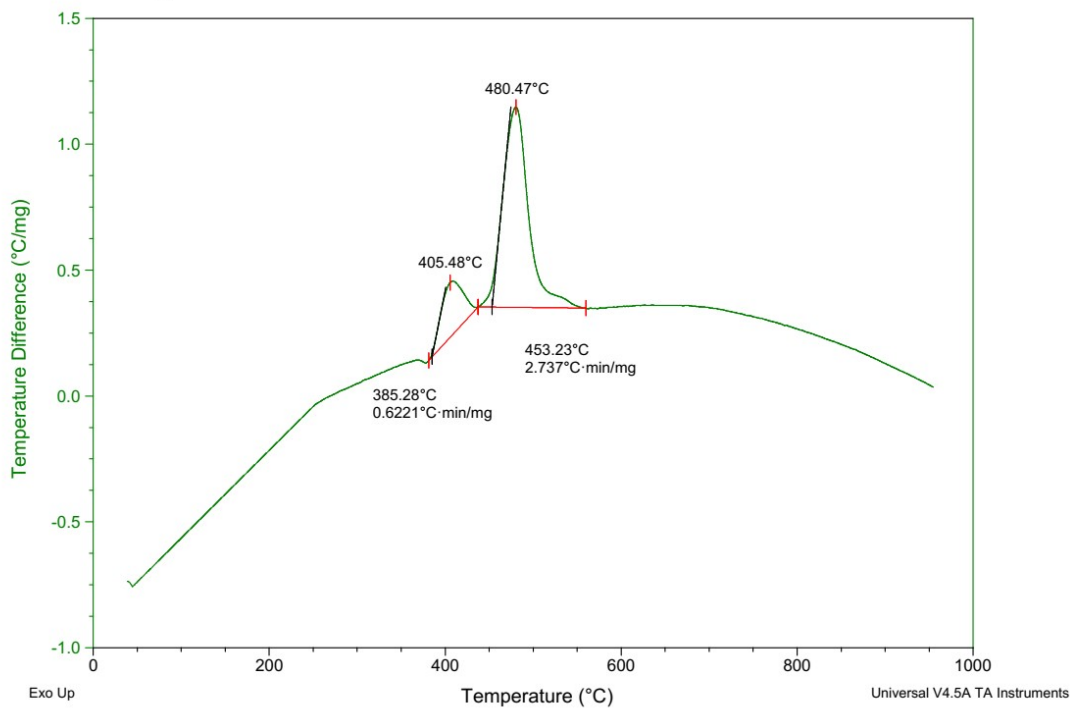


Figure S5. The TGA analysis of (a) FUM-153(Zn-H), (b) FUM-167(Cd-H), and (c) FUM-176(Cd-NH₂).

(a)



(b)



(c)

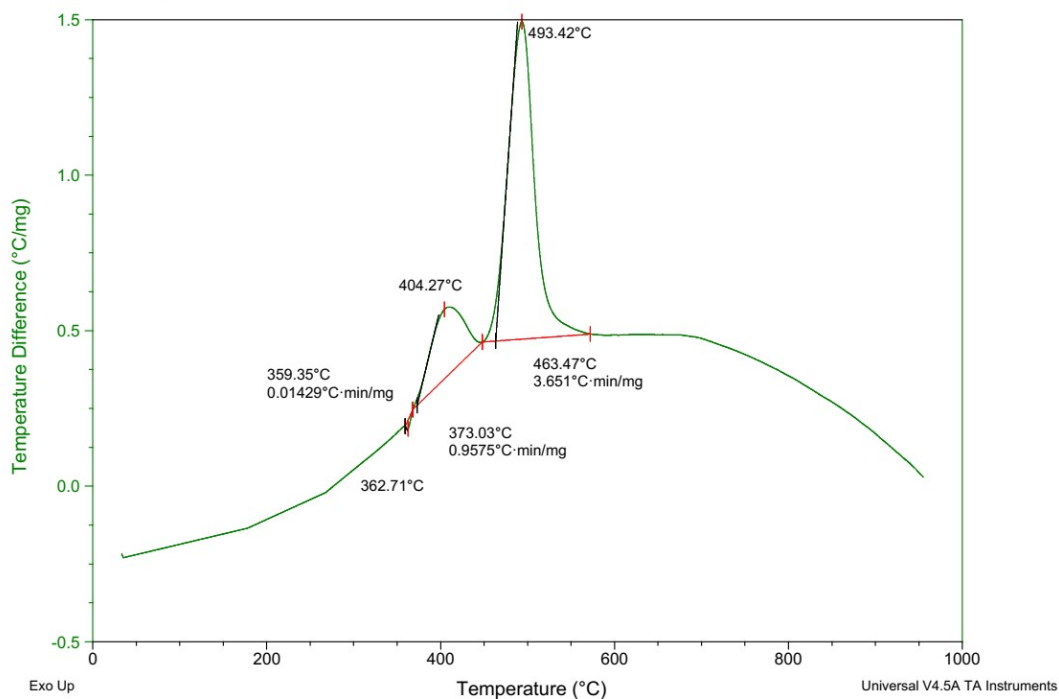


Figure S6. The DTA analysis of (a) FUM-153(Zn-H), (b) FUM-167(Cd-H), and (c) FUM-176(Cd-NH₂).

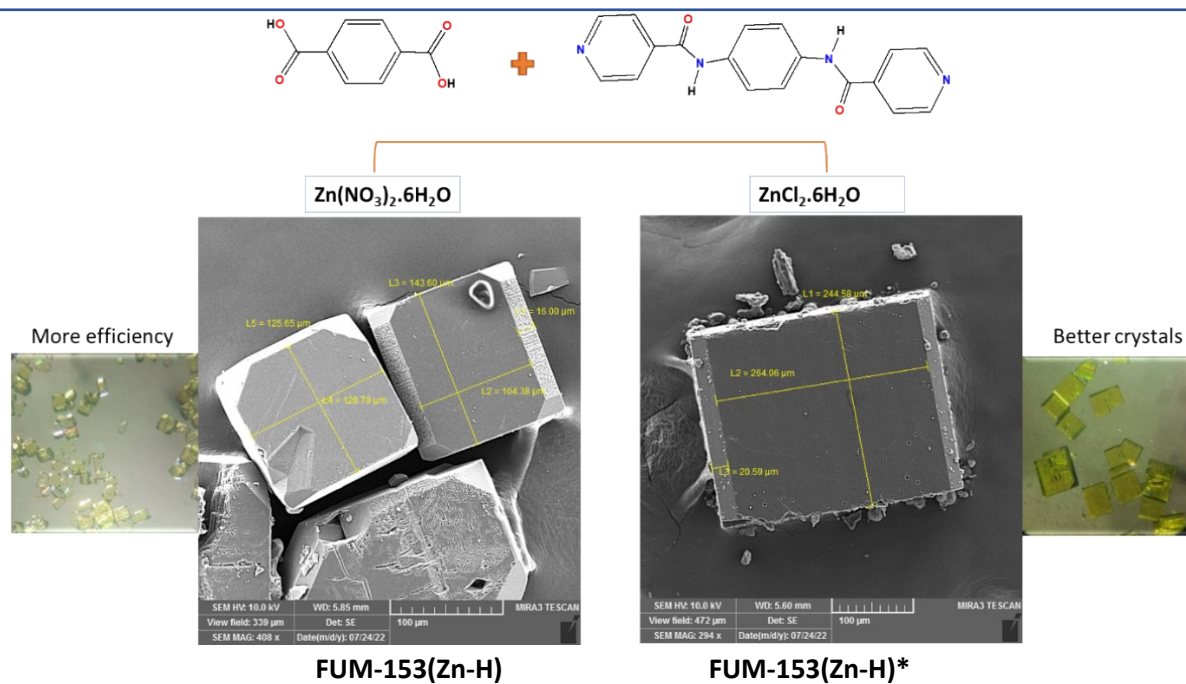


Figure S7. The representation of FT-SEM of FUM-153(Zn-H) and FUM-153(Zn-H)*.

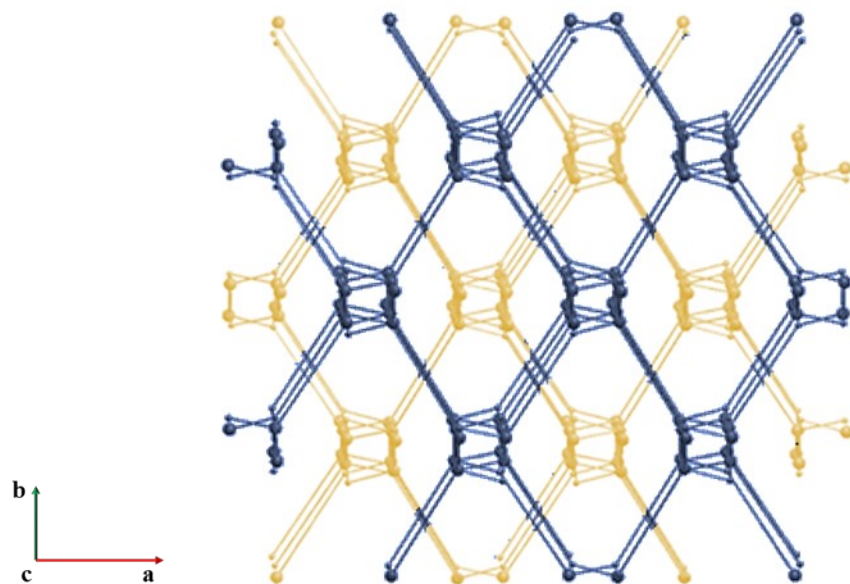


Figure S8. The representation of the 2-fold interpenetrating in **FUM-153(Zn-H)**.

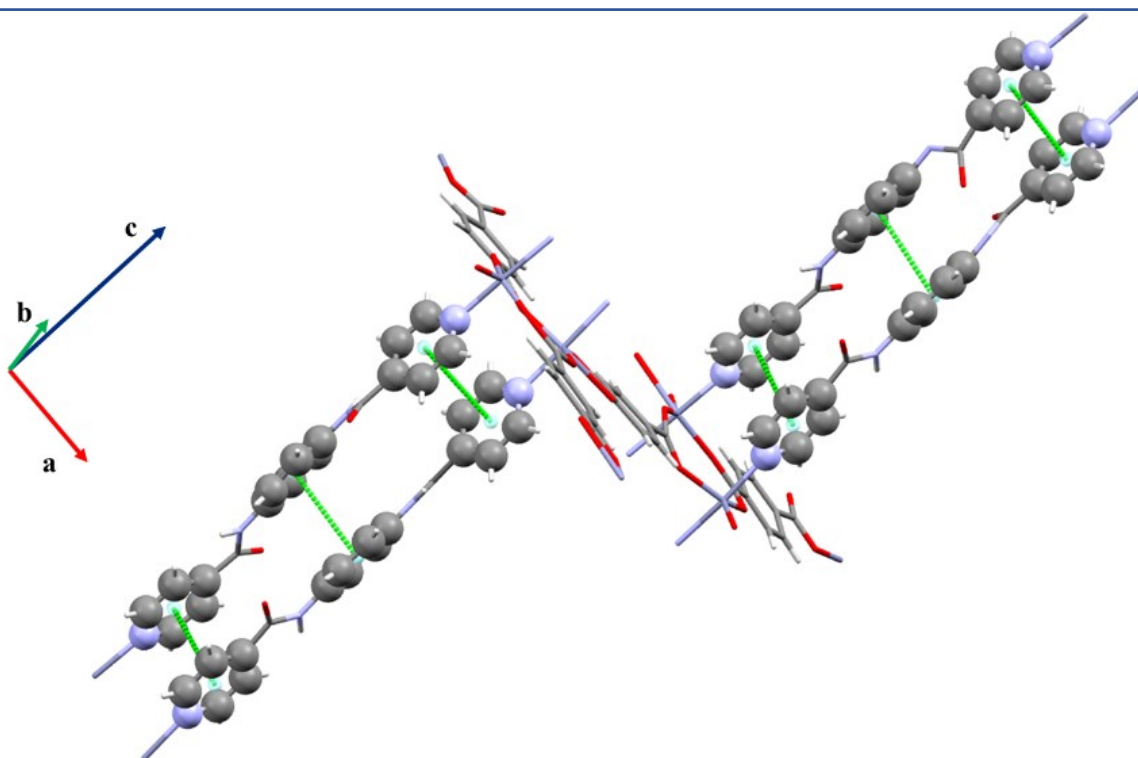


Figure S9. The representation of $\pi\cdots\pi$ interactions in **FUM-153(Zn-H)**.

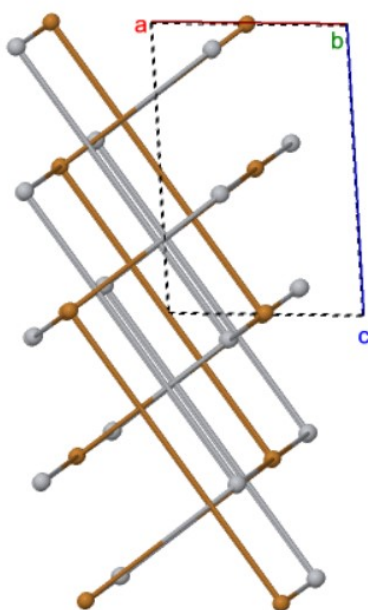


Figure S10. The representation of the 2-fold interpenetrating in **FUM-167(Cd-H)**.

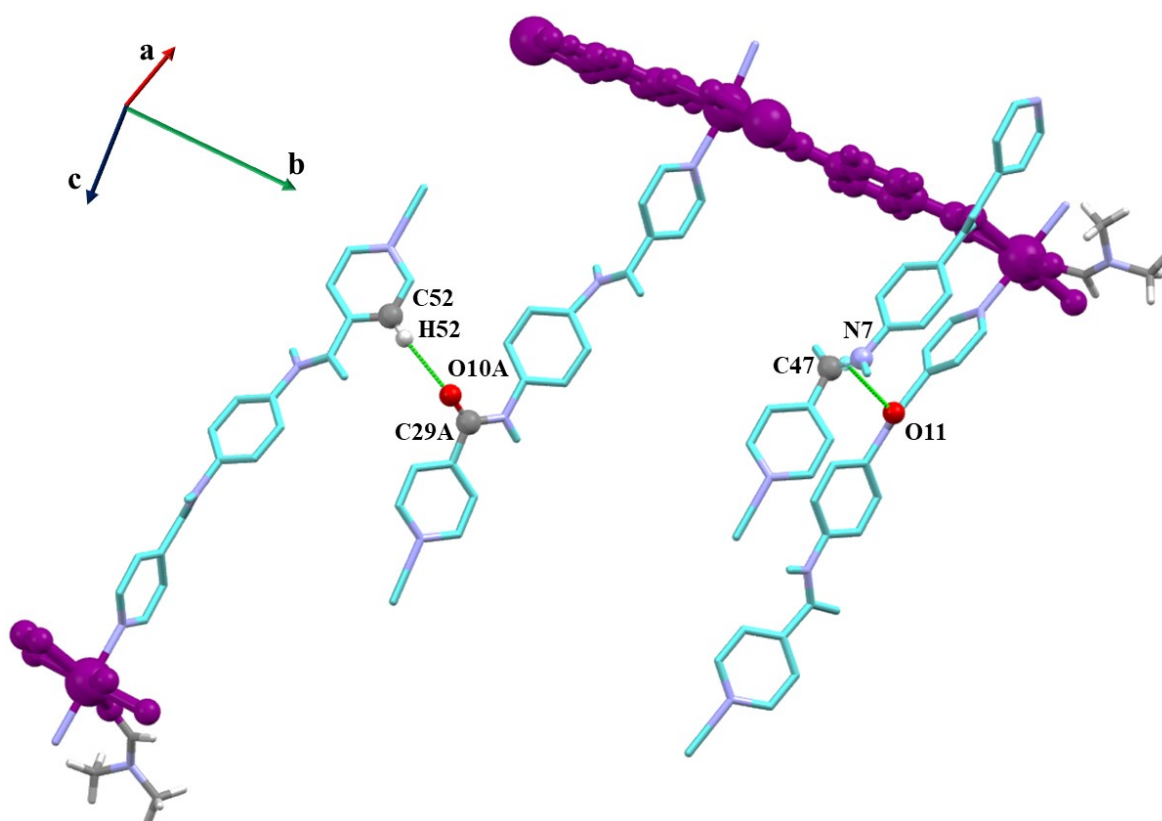


Figure S11. The representation of $C40 \cdots O11 \cdots C47$ $N7_{amide}$ and $C29A \cdots O10A \cdots H52$ $C52$ interactions interpenetrating in **FUM-167(Cd-H)**.

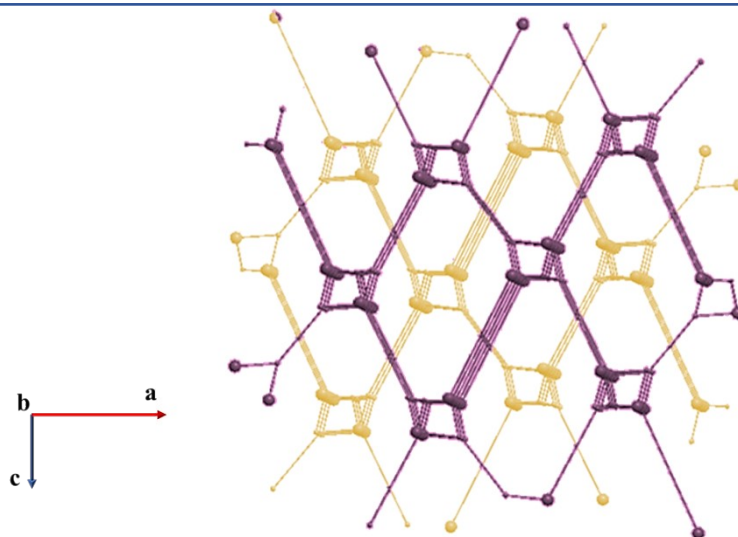


Figure S12. The representation of the 2-fold interpenetrating in **FUM-176(Cd-NH₂)**.

Chart S1. CH₄ and CO₂ gas adsorption result in the three FUMs.

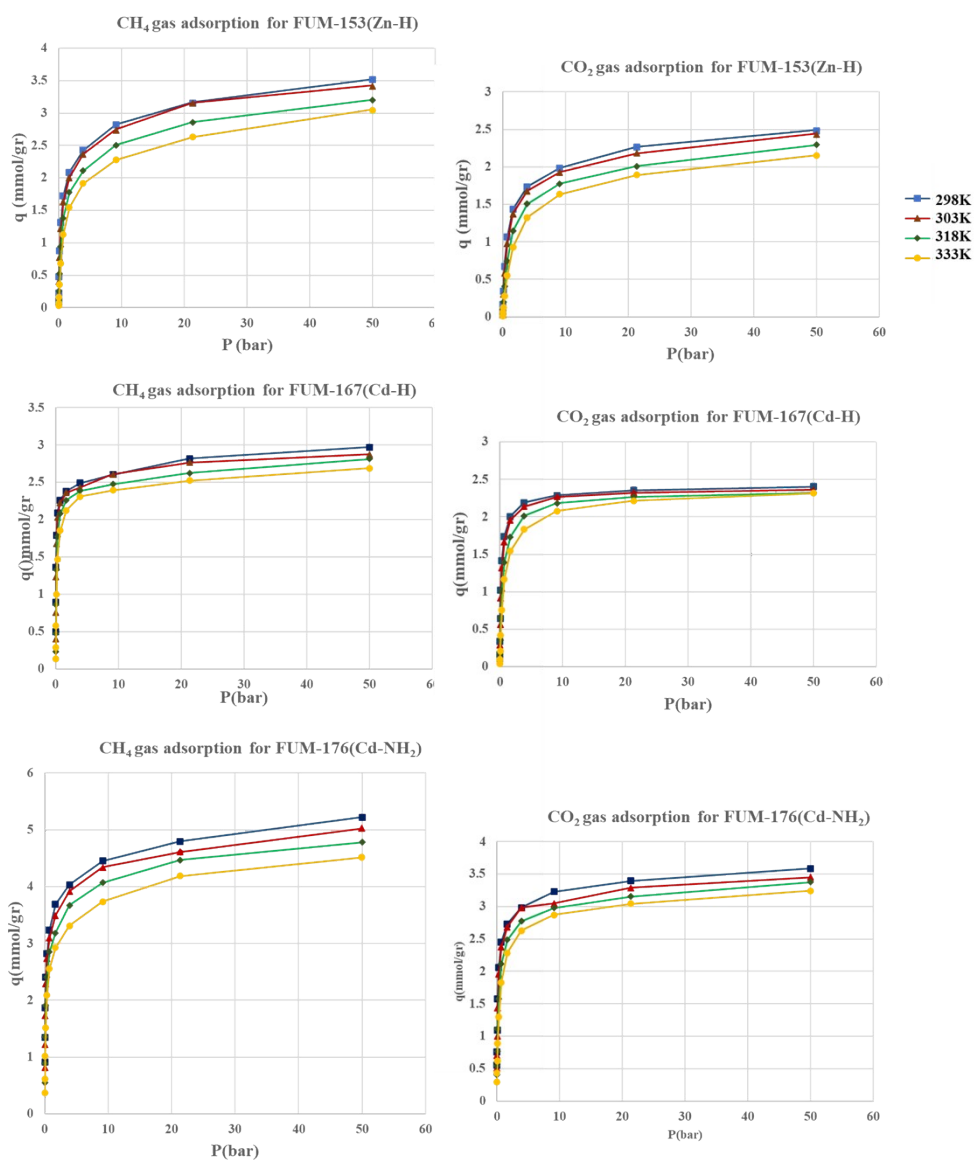


Table S1. The calculated gas adsorption results of all FUMs.

FUM-153(Zn-H)					
CH₄ adsorption	Temperature (K)	b (bar⁻¹)	q_{sat} (mmol/g)	Isosteric heat (kcal/mol)	ΔH_{ads} (kJ/mol)
	298	1.08	3.52	7.78	-12.86
	303	1.06	3.42	7.74	
	318	0.83	3.20	7.64	
	333	0.63	3.05	7.57	
FUM-153(Zn-H)					
CO₂ adsorption	Temperature (K)	b (bar⁻¹)	q_{sat} (mmol/g)	Isosteric heat (kcal/mol)	ΔH_{ads} (kJ/mol)
	298	0.83	2.49	6.71	-16.06
	303	0.75	2.44	6.69	
	318	0.56	2.29	6.65	
	333	0.42	2.15	6.62	
FUM-167(Cd-H)					
CH₄ adsorption	Temperature (K)	b (bar⁻¹)	q_{sat} (mmol/g)	Isosteric heat (kcal/mol)	ΔH_{ads} (kJ/mol)
	298	2.78	2.97	8.69	-6.58
	303	3.27	2.87	8.67	
	318	2.50	2.81	8.65	
	333	2.30	2.68	8.64	
FUM-167(Cd-H)					
CO₂ adsorption	Temperature (K)	b (bar⁻¹)	q_{sat} (mmol/g)	Isosteric heat (kcal/mol)	ΔH_{ads} (kJ/mol)
	298	3.78	2.40	8.18	-25.48
	303	3.68	2.35	8.19	
	318	2.23	2.32	8.20	
	333	1.33	2.31	8.21	
FUM-176(Cd-NH₂)					
CH₄ adsorption	Temperature (K)	b (bar⁻¹)	q_{sat} (mmol/g)	Isosteric heat (kcal/mol)	ΔH_{ads} (kJ/mol)
	298	1.85	5.22	8.79	-5.406
	303	1.88	5.02	8.75	
	318	1.74	4.78	8.72	
	333	1.48	4.51	8.67	
FUM-176(Cd-NH₂)					
CO₂ adsorption	Temperature (K)	b (bar⁻¹)	q_{sat} (mmol/g)	Isosteric heat (kcal/mol)	ΔH_{ads} (kJ/mol)
	298	2.52	3.58	8.02	-8.67
	303	2.57	3.45	8.00	
	318	2.02	3.37	8.02	
	333	1.81	3.24	8.03	